33rd Annual International Conference of the IEEE EMBS
Boston, Massachusetts USA, August 30 - September 3, 2011

# Sympathetic Neural Recruitment Patterns During the Valsalva Maneuver

Aryan Salmanpour, Maria F. Frances, Ruma Goswami and J. Kevin Shoemaker

*Abstract*— **Sympathetic nerve activity is an important regulator of blood pressure and blood flow in humans. Our understanding about how sympathetic neurons are recruited during baroreflex stress is limited. This paper investigates the sympathetic neural recruitment patterns during the Valsalva maneuver. Using microneurography, muscle sympathetic nerve activity was recorded in seven healthy subjects during baseline and the Valsalva maneuver. A new algorithm for detection and classification of action potentials was employed to study the differences between the recruitment of sympathetic neurons during baseline and the Valsalva maneuver. The data suggests that the Valsalva maneuver increases the number of spikes per sympathetic bursts and also recruits at least one additional new cluster of larger, faster conducting neurons. Also, action potential's latencies (i.e., inverse of conduction velocity) were shifted downward for all action potential clusters during this maneuver.**

## I. INTRODUCTION

Sympathetic nerve activity (SNA) plays a vital role in blood pressure regulation and blood pressure distribution. The SNA signal associated with blood pressure regulation can be recorded directly using Microneurography [1]. The human muscle sympathetic nerve activity (MSNA) is generated by multiple neurons supplying the vascular bed of muscle in human subjects. This signal is characterized by spontaneous burst activity of spikes (action potentials) that are time-locked with the cardiac cycle and separated by silent periods against a background of considerable gaussian noise. Analysis of these action potentials and their distribution provides information regarding the recruitment strategies employed by the central sympathetic nervous system in order to achieve the spontaneous activity and stress responses. Little is known about these neural recruitment patterns in sympathetic nervous system because of the lack of a proper spike detection algorithm for sympathetic neural recordings.

Recently, we developed a new spike detection technique that enables the identification and morphological classification of multiple vasomotor neurons contributing to sympathetic bursts [2]. We have applied our spike detection and classification technique during chemoreflex [3] and baroreflex [4] stresses to study neural recruitment patterns. The results of these studies indicated that there exists a fundamental pattern of recruitment of additional larger, faster conducting neurons as the sympathetic bursts become stronger (i.e., larger amplitude bursts). This pattern was observed during baseline conditions and was unaltered during the moderate level of baroreflex stress [4]. However, during strong baroreflex and chemoreflex stresses, otherwise silent sympathetic neurons are activated with greater probability in an order that appears to be based on neuronal size (from smallest to largest). It appears that a severe stress is required to provoke recruitment of these large and fast-conducting postganglionic axons.

The purpose of the current study was to examine further the neural recruitment patterns during the Valsalva maneuver. The Valsalva maneuver, a strong baroreflex stress, consists of a prolonged expiratory effort resulting in increased intrathoracic pressure, with concomitant decreased venous return and alterations in arterial pressure and heart rate. It increases the MSNA signal via baroreflex activation. Our approach was to apply our technique to extract action potential contents from extracellular sympathetic recordings during base-line and the Valsalva maneuver and classify these action potentials based on their peak-to-peak amplitude and their reflex latency (i.e., inverse of conduction velocity).

## II. MATERIALS AND METHODS

### A. Data acquisition and recording conditions

MSNA was recorded from the peroneal nerve of seven healthy subjects (three males, four females, $27 \pm 4$ yrs) during three minutes of baseline followed by two Valsalva maneuvers, separated by two minutes rest. During the two maneuvers, subjects were required to blow into sphygmomanometer tubing and hold the mercury column up to produce 35 mmHg pressure for a period of at least 30s.

Briefly for peroneal nerve recordings, a 200 $\mu m$ diameter, 35 mm long tungsten microelectrode tapering to an uninsulated 1 to 5 $\mu m$ tip was inserted transcutaneously into the peroneal nerve just posterior to the fibular head. A reference electrode was positioned subcutaneously 1-3 cm from the recording site. Neurograms were measured with a nerve traffic analysis system (662C-3, Bioengineering of University of Iowa, Iowa City, IA). The neural signal was preamplified with a gain of 1000 and further amplified with a gain of 75. This neuronal activity was then band-pass filtered (bandwidth of 700-2,000 Hz) and finally filtered MSNA was rectified and integrated. Integration is accomplished with a

This work was supported by Natural Science and Engineering Research Council of Canada (NSERC).

A. Salmanpour is with the Department of Electrical and Computer Engineering and Neurovascular Research Laboratory, Faculty of Health Sciences, University of Western Ontario, London, ON N6A 3K7, Canada asalmanp@uwo.ca

R. Goswami and M. F. Frances are with Neurovascular Research Laboratory, School of Kinesiology, Faculty of Health Sciences University of Western Ontario, London, ON N6A 3K7, Canada

J. K. Shoemaker is with Neurovascular Research Laboratory, School of Kinesiology, and Faculty of Physiology and Pharmacology, University of Western Ontario, London, ON N6A 5B9, Canada kshoemak@uwo.ca

leaky integrator typically set with a 0.1 s time constant. All signals were digitized with a data acquisition system (Powerlab software, AD Instruments Inc.) at a sampling rate of 10 kHz.

### *B. Integrated MSNA burst Analysis*

The strength of sympathetic activity was expressed both as number of bursts per 100 heartbeats (burst incidence) and burst per min (burst frequency). Reflex latency was determined as the time delay between the R-wave related to the burst (the previous R-wave in which the burst was observed) and the peak of the burst (the highest point of the integrated MSNA burst) [5]. Reflex latency was calculated for each burst and averaged for all detected bursts in each condition for each volunteer (mean reflex latency).

### *C. Action Potential Detection and Analysis*

Action potentials were detected and extracted from the filtered raw MSNA signal using the techniques developed previously [2]. Briefly, this technique uses a continuous wavelet transform (CWT) for action potential detection. The CWT used a "mother wavelet" that was adapted to an actual average action potential waveform constructed from physiological recordings of post-ganglionic sympathetic action potentials (i.e., matched mother wavelet had the same morphology as a physiological sympathetic action potential) [2]. The designing process involves a) detecting action potentials from the filtered raw MSNA signal and averaging them to build a mean action potential template and b) matching the amplitude and the phase of the new mother wavelet to that of the mean action potential template in the frequency domain [2].

The CWT with the matched mother wavelet was applied to the filtered MSNA to provide a wavelet coefficient between the signal of interest (i.e., an action potential) and the mother wavelet such that the wavelet coefficient was largest in the presence of the action potentials and negligible when applied to noise. Wavelet coefficients related to action potentials and noise were separated based on thresholding analysis [2]. The exact location of the negative peak for each action potential was then detected by isolating the largest supra-threshold wavelet coefficient. Using this location information the action potential waveforms were obtained from the original signal by putting the estimated location of action potentials in the center of a predefined window (3.2 ms). In this way, the amplitude and morphology of each extracted action potential remained unaltered. Extracted action potentials were then ordered based on peak-to-peak amplitude and histogram analysis was performed to separate action potentials into amplitude-based clusters based on Scott's Rule [6]. The Scott's rule proposes the optimal histogram bin width based on the sample size and an estimate of the standard deviation of the data. As such, the number of total clusters varied by subject.

The signal-to-noise ratio for a period of data was determined as the amplitude of the negative peak of the mean action potential over the standard deviation of the background noise (i.e. during sympathetic silence). Action potential latency (i.e., inverse of conduction velocity) was determined as the time delay between the R-wave of the electrocardiogram related to the burst of action potentials (i.e., the previous R-wave in which the burst of action potentials was observed) and the negative peak of the action potential waveform.

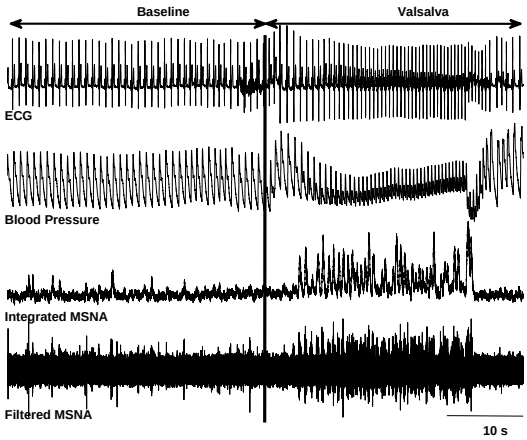


Fig. 1. A representative example of filtered raw and integrated muscle sympathetic nerve activity at rest and during the Valsalva maneuver.

TABLE I

POST-GANGLIONIC SYMPATHETIC ACTION POTENTIALS (AP) AND ACTION POTENTIAL CLUSTERS WITHIN SYMPATHETIC BURSTS DETECTED AT BASELINE AND DURING THE VALSALVA MANEUVER FOR EACH PARTICIPANT.

| | Baseline | | Valsalva | |
|---|---|---|---|---|
| Subject | AP/bursts | clusters/bursts | AP/bursts | clusters/bursts |
| 1 | 6 | 3 | 10 | 4 |
| 2 | 17 | 6 | 28 | 7 |
| 3 | 15 | 3 | 17 | 5 |
| 4 | 23 | 6 | 31 | 7 |
| 5 | 9 | 5 | 19 | 7 |
| 6 | 9 | 4 | 19 | 6 |
| 7 | 27 | 6 | 30 | 7 |
| Mean±SD | $15 \pm 8$ | $5 \pm 1$ | $22 \pm 8^*$ | $6 \pm 1^{\S}$ |

$^*P < 0.05$ $^{\S}P < 0.001$

### *Statistical Analysis*

Values are given as means $\pm$ STD. The effect of condition (baseline vs the Valsalva maneuver) was assessed using a two-tailed, paired, t test. Probability values $< 0.05$ were considered statistically significant.

## III. RESULTS

Corresponding filtered raw and integrated MSNA data were obtained for 190 s at baseline and 30 s of two Valsalva maneuvers for burst and action potential analysis. An example of the raw MSNA data at base-line and during the Valsalva maneuver is shown in Figure 1. Notice the reduced blood pressure and corresponding activation of sympathetic nerve activity. Compared with baseline, burst frequency ($15\pm 6$ vs. $34 \pm 6$ bursts.min$^{-1}$, $P < 0.001$) and burst incidence ($25 \pm 12$ vs. $45 \pm 5$ burst.100 heart beats$^{-1}$, $P < 0.05$) were

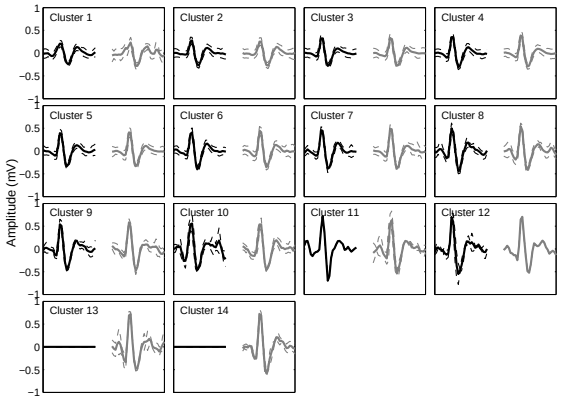


Fig. 2. Representation of mean post-ganglionic sympathetic action potential clusters detected at baseline shown with black color (61 bursts, 536 action potentials) and at Valsalva shown with gray color (27 bursts, 501 action potentials) in one participant. Solid and dashed lines represent means and standard deviations of cluster amplitudes. Clusters are binned based on peak-to-peak amplitude of each action potential.

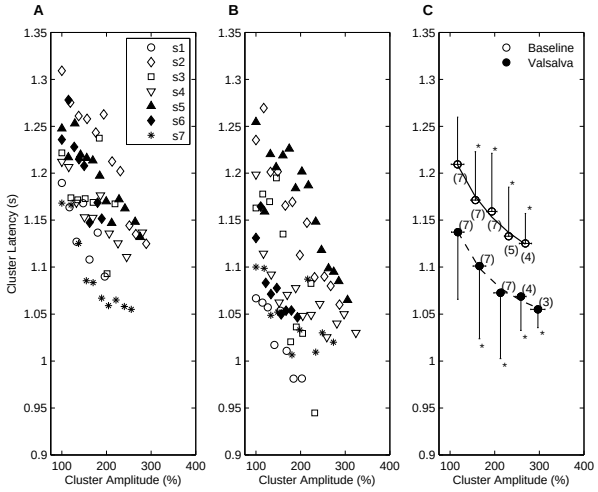


Fig. 3. Mean action potential latency for each cluster as a function of normalized cluster amplitude (cluster 1 = 100%) for each participant during baseline (A) and at the Valsalva maneuver (B). Mean cluster latency, binned across participants, as a function of normalized cluster amplitude during baseline and the Valsalva maneuver (C). Numbers indicate the number of subjects per bin. The decrease in cluster latency as a function of amplitude was fit with a modified exponential decay (see text)(solid-line base-line, dashed-line the Valsalva maneuver). * Latency significantly different from first bin, $P < 0.05$ in both baseline and the Valsalva maneuver.

increased in the Valsalva maneuver. Compared to baseline ($0.3 \pm 0.09$ vs. $0.46 \pm 0.13$ V; $P < 0.001$), relative raw burst amplitude was increased during the Valsalva maneuver. Also, the mean reflex latency was decreased during the Valsalva maneuver ($1.26 \pm 0.05$ vs. $1.17 \pm 0.04$ s; $P < 0.05$). For sympathetic action potential analyses, $49 \pm 26$ integrated sympathetic bursts consisting of a total of $665 \pm 344$ detected action potentials at baseline and $18 \pm 6$ bursts consisting of a total of $381 \pm 174$ detected action potentials during the Valsalva maneuver were analyzed per subject. Compared to baseline, action potentials per minute ($239 \pm 152$ vs. $676 \pm 221$ spikes.min$^{-1}$, $P < 0.001$) and action potentials per 100 heart beats ($404 \pm 274$ vs. $925 \pm 385$ spikes.100 heart beats$^{-1}$, $P < 0.05$) were increased during the Valsalva maneuver. Also, the mean action potential per sympathetic bursts was increased during the Valsalva maneuver (see Table I).

The number of distinct "clusters" of action potentials was increased at least by one new cluster when detected action potentials were binned based on peak-to-peak amplitude during the Valsalva maneuver and the same bin size was used for clustering at baseline, (see Table I). A representative example of detected sympathetic action potential clusters is shown in Figure 2. The extracellular action potential in human MSNA is triphasic and templates similar to those produced in the current study have been shown in [7]. At both baseline and the Valsalva maneuver action potential cluster latency decreased in each subject as an inverse function of peak-to-peak amplitude. The mean response was fitted using a modified exponential function ($R^2 = 0.9856$) at baseline and ($R^2 = 0.9879$) during the Valsalva maneuver. This exponential pattern was consistent with the well-defined relationship between action potential amplitude (proportional to the square of axon diameter) and conduction velocity [8] (see Figure 3). It was observed that the whole latency-size profile shifted downward around 73 ms during the Valsalva maneuver as the integrated mean reflex latency decreased significantly around 90 ms. The decrease in mean reflex latency of the integrated bursts during the Valsalva maneuver was also reported in [9].

The relationship between the occurrence of individual action potential clusters as a function of burst amplitude in one subject is shown in Figure 4A during baseline and in Figure 4B during the Valsalva maneuver. In general, action potential clusters present at rest were also present during the Valsalva maneuver. However, there were some new clusters (maximum 2 clusters) during the Valsalva maneuver that were not present during baseline condition. Also, the larger action potential clusters tended to fire within larger bursts but not smaller bursts.

## IV. CONCLUSIONS

In this paper, sympathetic action potential contents (i.e., recruitment patterns of sympathetic neurons) were compared during baseline and the Valsalva maneuver. In general, both baseline and the Valsalva maneuver showed a hierarchical recruitment strategy whereby the larger action potentials are recruited with a lower probability and, once recruited, contribute to the larger integrated MSNA burst. It was observed that the number of action potentials per sympathetic bursts was increased during the Valsalva maneuver; moreover, when detected action potentials were classified based on their peak-to-peak amplitudes, one or two new clusters showed up during the Valsalva maneuver. This trend was observed in all subjects (see Table I). The new clusters exhibited shorter latency. Also, the whole latency-size profile of action potentials (see Figure 3) was shifted significantly downward during the Valsalva maneuver.

Thus, incorporation of this analytical approach has exposed, for the first time, a unique ability of the sympathetic

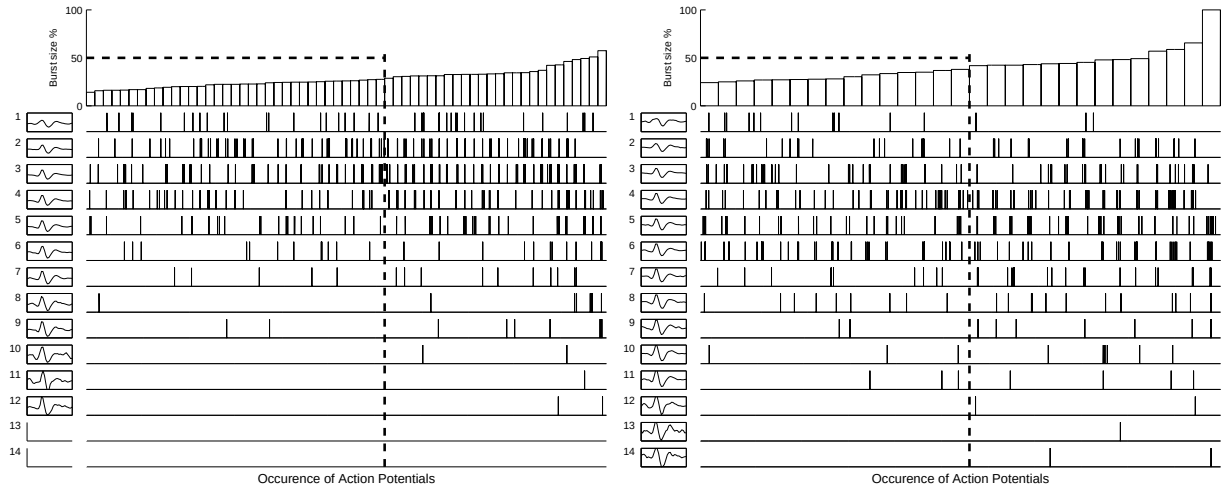


(A) Baseline (B) Valsalva

Fig. 4. The relationship between the occurrence of individual action potential clusters as a function of burst amplitude in one subject during baseline (A) and the Valsalva maneuver (B). In both section A and B, integrated sympathetic bursts are ordered by burst size where 100 % represents maximum burst size during the Valsalva maneuver. Below the sympathetic burst size, occurrences of post-ganglionic sympathetic action potentials as a function of integrated burst size are indicated for each action potential cluster (left panel). Notice that large action potential clusters are predominately recruited at larger bursts. Data presented are from the same participant presented in Figure. 2. (black and gray clusters for baseline and the Valsalva maneuver, respectively). Notice that the firing pattern of action potentials is similar during baseline and the Valsalva maneuver where large clusters occur during the large bursts. Also two new clusters (cluster 13 and 14) exist during the Valsalva maneuver but not during baseline.

nervous system to alter its recruitment patterns acutely in a manner that includes both the addition of new faster conducting neurons but also, and most notably, in the ability to reduce reflex latency of all action potentials. It is not clear what caused the systematic shift in reflex latency during the Valsalva maneuver that results in an earlier recruitment of action potentials of all different sizes. Possible scenarios for the reflex latency change are 1) existence of more than one central pathway involved in the baroreflex regulation of MSNA and/or 2) altered central processing time (see [9]). Another possible scenario is that the larger amplitude action potentials could be the result of summation of any two medium size action potentials that fire at the same time [10]. We believe that while this could be possible, it is unlikely as per our earlier analysis [2].

The current approach for action potential detection in MSNA bursts provides information on the size and latency of action potentials within MSNA bursts. A limitation of the approach is that it cannot be determined whether separate action potentials with the same shape (i.e., size) are from a single neuron or multiple neurons. Generally, those clusters active during baseline continued to be active during the Valsalva maneuver. However, whether or not these are the same neurons is not known. All that can be said here is that action potentials of similar sizes are present both at rest and during the Valsalva maneuver.

In conclusion, we showed the potential application of our action potential detection and classification technique for studying the recruitment patterns of sympathetic neurons during the Valsalva maneuver.

## REFERENCES

[1] K. E. Hagbarth and A. B. Vallbo, "Pulse and respiratory grouping of sympathetic impulses in human muscle nerves," *Acta physiol scand,* vol. 74, pp. 96-108, 1968.

[2] A. Salmanpour, L. J. Brown, J. K. Shoemaker, "Spike detection in human muscle sympathetic nerve activity using a matched wavelet approach," *J Neurosci Methods,* vol. 193, pp. 343-355, 2010.

[3] C. D. Steinback, A. Salmanpour, T. Breskovic, Z. Dujic, and K. J. Shoemaker, "Sympathetic neural activation: an ordered affair," *J Physiol,* vol. 588, pp. 4825-4836, 2010.

[4] A. Salmanpour, L. J. Brown, C. D. Steinback, C. W. Usselman, R. Goswami and J. K. Shoemaker, "Relationship between size and latency of action potentials in human muscle sympathetic nerve activity," *J Neurophysiol,* vol. 105, pp. 2830-2842, 2011.

[5] J. Fagius, B. G. Wallin, "Symphatetic Reflex Latencies and conduction velocities in normal man," *J Neurol Sci,* vol. 47, pp. 433-448, 1980.

[6] D. W. Scott, "On optimal and data-based histograms," *Biometrika,* vol. 66, pp. 605-610, 1979.

[7] V. G. Macefield, B. G. Wallin, A. B. and Vallbo, "The discharge behaviour of single vasoconstrictor motoneurones in human muscle nerves," *J Physiol,* vol. 481, pp. 799-809, 1994.

[8] H. P. Clamann, E. Henneman, "Electrical measurement of axon diameter and its use in relating motoneuron size to critical firing level," *J Neurophysiol,* vol. 39, pp. 844-851, 1976.

[9] J. Fagius, G. Sundolf, B. G. Wallin, "Variation of symphatetic reflex latency in man," *J Auton Nerv Syst,* vol. 21, pp. 157-165, 1987.

[10] M. C. Andresen and M. Yang, "Interaction among unitary spike trains: implications for whole nerve measurements," *Am J Physiol,* vol. 256, pp. R997-1004, 1989.